Brain Stimulation 12 (2019) 1143–1150

Contents lists available at ScienceDirect

Brain Stimulation

journal homepage: http://www.journals.elsevier.com/brain-stimulation

Focused ultrasound-induced blood brain-barrier opening enhanced vascular permeability for GDNF delivery in Huntington's disease mouse model

Chung-Yin Lin [a, b], Chih-Hung Tsai [c], Li-Ying Feng [d], Wen-Yen Chai [c], Chia-Jung Lin [c], Chiung-Yin Huang [d], Kuo-Chen Wei [d], Chih-Kuang Yeh [e], Chiung-Mei Chen [f, *], Hao-Li Liu [a, c, d, **]

[a] Medical Imaging Research Center, Institute for Radiological Research, Chang Gung University/Chang Gung Memorial Hospital, Taoyuan, 333, Taiwan
[b] Department of Nephrology and Clinical Poison Center, Chang Gung Memorial Hospital, Taoyuan, 333, Taiwan
[c] Department of Electrical Engineering, Chang Gung University, Taoyuan, 333, Taiwan
[d] Department of Neurosurgery, Chang Gung Memorial Hospital, Linkou Medical Center and College of Medicine, Chang Gung University, Taoyuan, 333, Taiwan
[e] Department of Biomedical Engineering and Environmental Sciences, National Tsing Hua University, Hsinchu, 300, Taiwan
[f] Department of Neurology, Chang Gung Memorial Hospital, College of Medicine, Chang Gung University, Taoyuan, 333, Taiwan

ARTICLE INFO

Article history:
Received 6 October 2018
Received in revised form
30 January 2019
Accepted 25 April 2019
Available online 27 April 2019

Keywords:
Focused ultrasound
Gene therapy
Blood-brain barrier opening
GDNF
Huntington's disease

ABSTRACT

Background: Huntington's disease (HD) is an autosomal dominant neurodegenerative disorder caused by a CAG trinucleotide repeat expansion in the gene encoding the huntingtin (Htt) protein, which results in a protein containing an abnormally expanded polyglutamine (polyQ) sequence. The expanded polyQ in the Htt protein is toxic to brain cells. No therapy exists to delay disease progression.
Methods: This study describes a gene-liposome system that synergistically applied focused ultrasound (FUS)-blood-brain barrier (BBB) opening for rescuing motor and neuropathological impairments when administered from pre to post-symptomatic transgenic mouse models of HD. DPPC liposomes (LPs) are designed to carry glia cell line-derived neurotrophic factor (GDNF) plasmid DNA (GDNFp) to form a GDNFp-liposome (GDNFp-LPs) complex. Pulsed FUS exposure with microbubbles (MBs) was used to induce BBB opening for non-viral, non-invasive, and targeted gene delivery into the central nervous system (CNS) for therapeutic purposes.
Results: FUS-gene therapy significantly improved motor performance with GDNFp-LPs + FUS treated HD mice equilibrating longer periods in the animal behavior. Reflecting the improvements observed in motor function, GDNF overexpression results in significantly decreased formation of polyglutamine-expanded aggregates, reduced oxidative stress and apoptosis, promoted neurite outgrowth, and improved neuronal survival. Immunoblotting and histological staining further confirmed the neuroprotective effect from delivery of GDNF genes to neuronal cells.
Conclusions: This study suggests that the GDNFp-LPs plus FUS sonication can provide an effective gene therapy to achieve local extravasation and triggered gene delivery for non-invasive *in vivo* treatment of CNS diseases.

Introduction

Huntington's disease (HD) is an inherited disorder characterized by neuronal dysfunction and degeneration in cerebral cortex and striatum [1]. A CAG trinucleotide repeat expansion leads to the production of an abnormally long polyglutamine (polyQ) sequence of the huntingtin (Htt) protein [1,2]. Htt is highly expressed in the brain, particularly in the cerebral cortex and striatum [3]. Expanded

* Corresponding author. Neurology, Chang Gung Memorial Hospital, Taoyuan, Taiwan, 333.
** Corresponding author. Department of Electrical Engineering, Chang Gung University, Taoyuan, 333, Taiwan.
E-mail addresses: cmchen@cgmh.org.tw (C.-M. Chen), haoliliu@mail.cgu.edu.tw (H.-L. Liu).

https://doi.org/10.1016/j.brs.2019.04.011
1935-861X/

polyQ is toxic to brain cells [4]. The pathological hallmark of HD is brain atrophy that is mainly in the cortex and striatum, and restrict particularly to the progressive loss of medium-sized striatal medium-sized spiny neurons and cortical pyramidal neurons [5,6]. Moreover, chronic mutant Htt (mHtt) expression alters the neurovasculature by increasing cerebral blood volume, reducing vessel density, and blood-brain barrier (BBB) permeability in animal models and clinical patients [7–9]. The endothelial cells form BBB, the main elements of the neurovascular unit, that restrict paracellular and transcellular entry into the CNS [10,11].

There is currently no effective treatment that can retard or reverse the progression of HD. Target compounds such as neurotrophic factors (NFs) have been considered to play a potentially significant role in neuroprotection in HD [12–14]. NFs, supporting the survival of CNS neurons, have demonstrated their reduced availability in neurological disorders, and insufficiency of neural NFs supply thereby promotes neurodegeneration [15–17]. More recently, gene therapy provides exciting potential for improved therapeutic efficacy [18]. Glial cell line-derived neurotrophic factor (GDNF) is one of the best-studied NFs and has been shown to promote the growth, development, survival, and trophic plasticity of striatal neurons [19–21]. In addition, GDNF has been found to be neuroprotective against toxin-induced neurodegeneration [22]. Direct local delivery of GDNF to the CNS can be performed using a catheter or needle [12,23], but this invasive approach is associated with the risk of neurologic damage, bleeding, and infection, and also requires multiple bi-monthly injections to ensure sustained benefit [12]. Noninvasive gene delivery via systemic routes to the brain encounters several major limitations. One limitation is that naked plasmid genes are quickly degraded by endogenous nucleases and are rapidly cleared by the reticuloendothelial system (RES) [24–26]. A second limitation is that the targeting compounds such as GDNF into CNS can be hampered due to blockage by the BBB. Studies have shown that HD gradually develops BBB integrity impairment with age, leading to profound disturbance of brain homeostasis [10,15–17]. Previous studies have shown the correlation of the neurovasculature impairment and pathologically-developed BBB breakdown and have some implications for identifying potential HD therapies in the future [7,15,27].

The use of focused ultrasound (FUS) to transiently open the BBB for noninvasive delivery of therapeutic genes has been investigated [26,28–31]. The combination of burst FUS exposure in the presence of microbubbles (MBs) effectively enhances cavitation to temporally disrupt the BBB. FUS-mediated BBB opening also allows therapeutic agents to deposit at specific sites noninvasively, with the BBB recovery few hours after the procedure [32–37]. We have previously shown that the synergistic use of FUS-BBB opening with GDNF-gene-vector to perform noninvasive GDNF gene delivery, which could enhance treatment efficacy in a Parkinson's disease (PD) mouse model [26,30,31]. We therefore hypothesize that GDNF gene delivery to specific brain region with FUS-mediated BBB opening has beneficial effects on HD transgenic mice.

This study aims to verify that self-designed gene vector, a liposome-containing plasmid DNA formulation, can be used in conjunction with FUS-BBB opening to promote CNS GDNF gene delivery for HD treatment. Fig. 1 shows the proposed strategy concept. FUS exposure would induce MB oscillation in blood vessels and locally amplify acoustic cavitations to promote GDNF gene penetration and delivery into the HD brain. MRI was used to follow HD anatomical regional atrophy of normal and diseased mice. Immunohistochemical analysis was conducted to examine the formation of neuronal aggregates in HD mice over time. Biophysical/biochemical analysis was conducted to characterize the consequence of the GDNF gene-delivery.

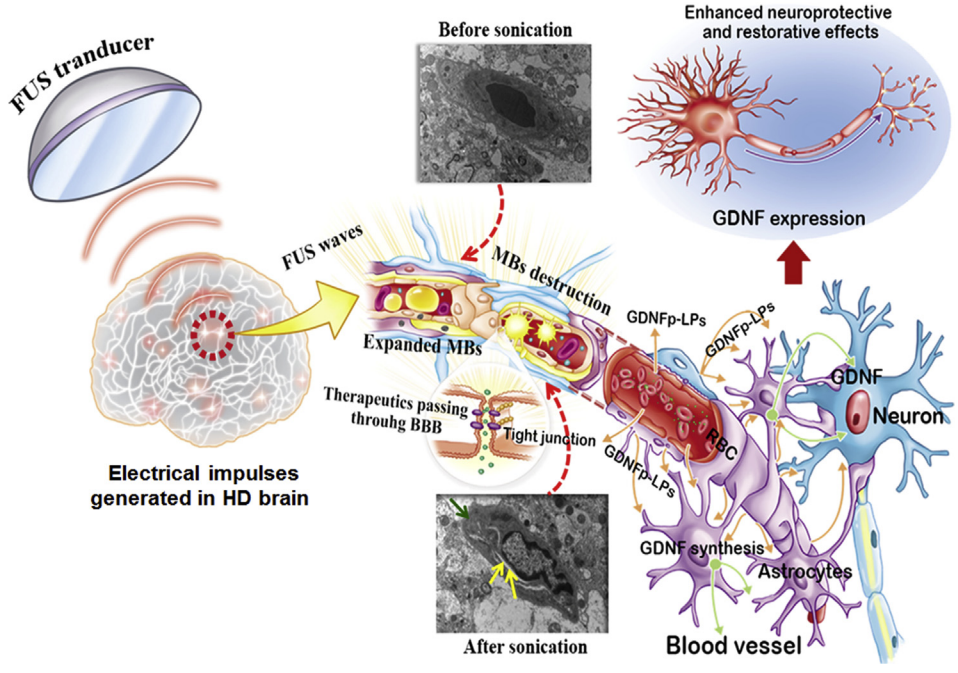

Fig. 1. Schematic representation of FUS-mediated GDNFp-LPs delivery for treatment of HD transgenic mice. BBB ultrastructure alterations in the ipsilateral striatum at 2 h after FUS-BBB opening. The regular capillary lumen, integrity base membrane, and normal extracellular space are observed prior to FUS exposure (Before sonication). The swelling of end-feet (green arrow), disrupted base membrane, narrowed capillary lumen and enlarged extracellular space (yellow arrows) are observed at 2 h after FUS exposure (After sonication). The yellow circles represent microbubbles (MBs), small green circles represent glia cell line-derived neurotrophic factor plasmid DNA-liposomes (GDNFp-LPs), and red circles represent red blood cells (RBC). Scale bar, 2 μm. FUS = focused ultrasound; BBB = blood-brain barrier. (For interpretation of the references to colour in this figure legend, the reader is referred to the Web version of this article.)

Materials and methods

See Supplementary Materials and Methods.

Results

Design of LP-encapsulated pDNA and in vitro validation for gene delivery

To achieve cell-specific targeting and to overcome the barriers to cytosolic and nuclear delivery, condensed pDNA encapsulated in LPs is crucial to maintaining gene delivery efficiency through intravenous administration. LPs that encapsulated GDNF-, HttQ25-, and HttQ109-pDNA were formulated. After encapsulating pDNA within LPs and removing the un-encapsulated pDNA by spin column, the amount of encapsulated pDNA was calculated from the absorbance of pDNA in the resulting pDNA-LPs. Fig. 2 shows the characteristics of the pDNA-LPs used in this study. Fig. 2A shows the zeta potential of pDNA/pDNA-LPs with a negatively charged surface, implying only minor changes of electrical potential of DPPC LPs. Fig. 2B shows the size distribution of L-HttQ25, L-HttQ109, and GDNFp-LPs with a mean diameter approximately 150 nm. Fig. 2C shows the cryo-TEM images of L-HttQ25, L-HttQ109, and GDNFp-LPs. Apparently, the DPPC-based LPs can trap hydrophilic pDNA and interact with pDNA to form pDNA-LPs. The mean size was approximately 150 nm for pDNA-LPs.

To analyze if ultrasound exposure can induce polyQ-containing Htt expression and form aggregates *in vitro*, the disease-inducing Htt protein exon 1 fragment (L-HttQ109) and its wild-type counterpart (L-HttQ25) constructs were used in transient transfection experiments on N2A cells. As shown in Fig. 2D, the red fluorescence (1C2) signals was uniformly and evenly distributed throughout the cytoplasm and nucleus in L-HttQ25 and L-HttQ109 cells. The red fluorescence was also generally distributed evenly throughout the cytoplasm, with small aggregates in cytoplasm and large aggregates in nucleus of L-HttQ109 cells after ultrasound exposure. In contrast, HttQ25-expressing cells contained no visible aggregates and instead expressed a relatively homogeneous intracellular distribution at the time point examined (middle column). This aggregation was found in most HttQ109-expressing cells after ultrasound induction over 48-h period.

In vivo BBB opening and paracellular permeability

The efficiency of FUS exposure in conjunction with microbubbles to temporally open the BBB at striatum of R6/2 HD mice was evaluated. Fig. 3A shows a typical example of a contrast-enhanced MRI and the corresponding HE stained brains to confirm BBB-opening efficacy via the proposed system. Enhanced T1-weighted images confirm the BBB-opening scale under 0.33-MPa exposure pressure. Subtracted MR images showed enhancive signal intensity in the surrounding striatum regions, suggesting Gd-DTPA leakage. The HE-stained brain sections with 0.33-MPa exposure pressure confirmed no potential capillary/brain tissue damage. The 0.33-MPa exposure level was thus used for the following R6/2 HD mice treatments. In addition, BBB integrity was also evaluated by detecting EB extravasation after FUS-BBB opening. As shown in Fig. 3B, EB extravasation was significantly increased in the sonicated brains of R6/2 HD mice and WT mice. The amounts of EB deposited in the sonicated tissues were 0.36 ± 0.13, 0.45 ± 0.12, and 0.46 ± 0.14 μg/g for 6, 12, and 18-week-old R6/2 HD mice, and 0.6 ± 0.13, 0.41 ± 0.11, and 0.48 ± 0.13 μg/g for 6, 12, and 18-week-old WT mice. The permeability of EBs in the rostral regions for FUS-BBB opening was significantly higher than under non-sonicated conditions, and the difference is statistically significant ($^{***}P < 0.005$ and $^{**}P < 0.01$) for all age groups except R6/2 HD mice at 18 weeks of age.

The EB extravasation experiment showed a tendency in increase of BBB permeability in R6/2 HD mice compared to WT at 18-weeks of age. It is also noted that FUS-BBB opening did not enhance significantly the BBB permeability in R6/2 HD mice at 18-weeks of age. To determine if BBB permeability occurs relative to HD progression, we examined the kinetic changes induced by FUS exposure via DCE-MRI analysis. DCE-MR scanning was performed to evaluate the effect of dynamic BBB permeability changes on the basis of regions of interest drawn in anatomically identical positions in Fig. 3C. The BBB-opened region was clearly identified as the region of Gd-DTPA penetration into the striatum, implying that BBB-opening effect was involved. DCE-MR images were further investigated for dynamic permeability changes to analyze the kinetic parameters of an ROI at the BBB-opened regions between 18-week-old R6/2 HD and WT mice. It is noted that Ktrans level is higher in R6/2 HD mice compared to the WT mice, indicating

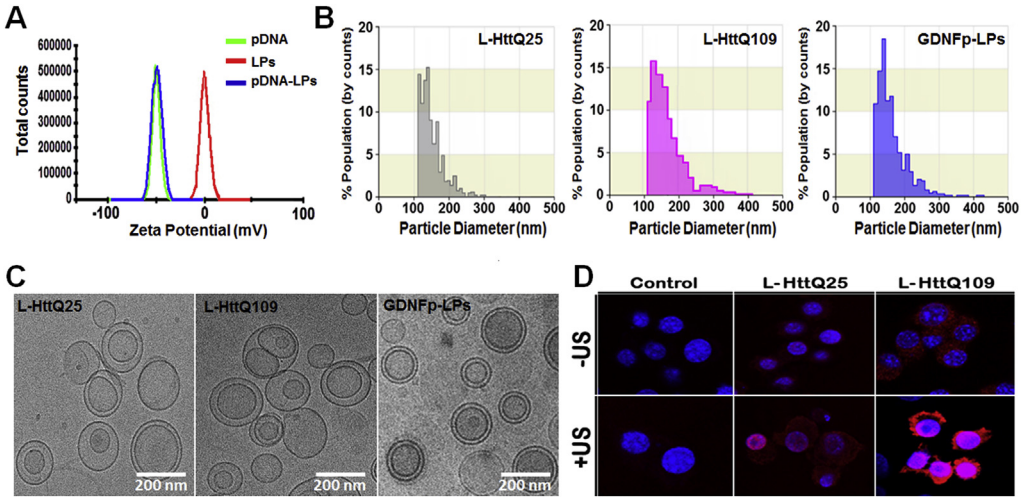

Fig. 2. Characteristics of the GDNFp-LPs, the L-HttQ25, and the L-HttQ109 nanoparticles used in this study. (A) Particle zeta potential; (B) particle size distribution; and (C) particle morphologies. (D) Immunocytochemical staining (1C2 antibody for detection of huntingtin) of N2A cells transfected with L-HttQ25 or L-HttQ109 with or without ultrasound (US) sonication. After 2 days of induction, expression of HttQ109 fragment leaded to aggregate formation in N2A cells transfected with L-HttQ109 by US whereas clones expressing HttQ25 showed no detectable aggregate formation.

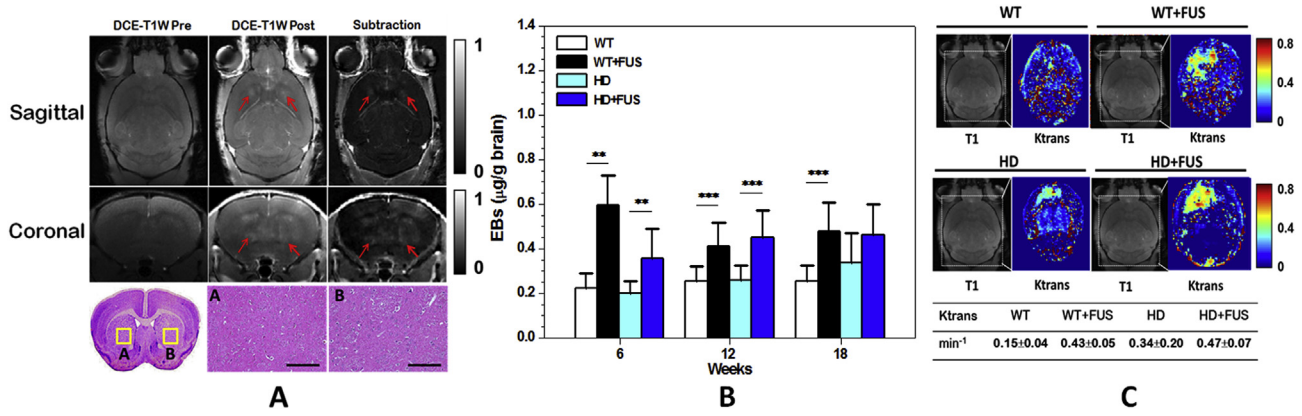

Fig. 3. (A) Representative MR images before and after FUS-BBB opening in 6-week-old R6/2 HD mice. T1-weighted images of sagittal and coronal regions (left column); Gd-DTPA contrast-enhanced T1-weighted images of sagittal and coronal regions (middle column); subtracted after and before Gd-DTPA injection T1 images of sagittal and coronal regions (right column), corresponding HE stained section. (B) The amount of EB extravasation before and after FUS-BBB opening in both WT and R6/2 HD mice over time. (C) The values of Ktrans maps before and after conducting FUS-BBB opening in both 18-week-old WT mice and R6/2 HD mice. Parameters were as follows: acoustic pressure, 0.33 MPa; frequency, 500 kHz; burst duration, 10 msec; PRF, 1 Hz; duty cycle, 1%; total exposure time, 30-sec at contralateral hemisphere and another 60-sec at ipsilateral hemisphere; and MB dose, SonoVue® 0.1 mg/kg. Data represent means ± S.D of three independent experiments. Significant difference was denoted as "*", "***", and "****" to respectively represent $P < 0.05$, $P < 0.01$, and $P < 0.005$ (Mann-Whitney U test).

impaired BBB in HD mice at 18-weeks of age. In the WT mice, we observed a peak value of Ktrans of 0.43 ± 0.05 min^{-1} after FUS exposure from static 0.15 ± 0.04 min^{-1}, whereas Ktrans of 0.47 ± 0.07 min^{-1} from static 0.34 ± 0.20 min^{-1} in R6/2 HD mice. R6/2 HD mice had a higher Ktrans level after FUS-BBB opening at 18-weeks of age. Similarly, EB extravasation showed increased permeability after FUS-BBB opening, although not statistically significant in 18-week-old R6/2 HD brains. Taken together the results support the plausibility of using FUS to open the BBB either in WT or R6/2 HD mice, but the BBB opening is less effective in late HD mice.

FUS CNS gene delivery ameliorated aggregation, oxidative stress, inflammation and neurodegeneration in HD transgenic mice

The time course of the R6/2 HD mice including the schedule of FUS treatment, rotarod, as well as histological analysis was summarized in Fig. 4A. The mice were grouped into sham, GDNFp-LPs only, FUS only, and GDNFp-LPs + FUS. To study the pathological changes after the FUS CNS gene delivery treatment, a series of immunohistochemical staining were performed, including protein aggregation, oxidative stress, and inflammatory and apoptosis markers. Fig. 4B shows the examination of the protein expression patterns and the spatial distributions of cell types in various animal groups in 14-week-old mice. It shows WB analysis results for the GDNF protein expression among various experimental groups. Using the readout from the sham group as a baseline, significant GDNF protein expressions was observed in the GDNFp-LPs + FUS animal group. This suggests that FUS-BBB opening successfully delivered GDNFp-LPs into brain target region, and transfected and eventually transduced GDNF expression.

Microscopically visible huntingtin protein aggregates serve as important indicator in HD progression (Fig. 4C 1st and 2nd columns). Significant reductions in Htt aggregates in cortex/striatum

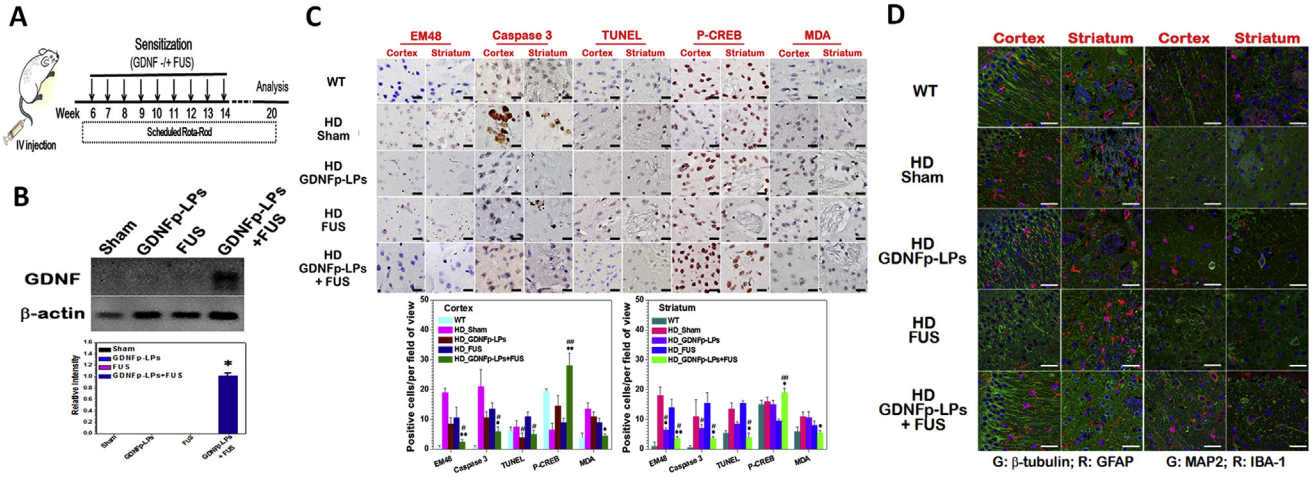

Fig. 4. (A) Timeline of the study design and schematic of the mouse treatment-procedure. (B) Levels of neuronal GDNF expression after 9 weeks of treatment. (C) Immunodetection of tissue slides from WT mice and HD mice with and without FUS-gene therapy. Microscopic assessment of protein aggregates, Caspase 3, TUNEL, P-CREB, and MDA numbers. (D) Immunohistochemical localization of β-tubulin, GFAP, MAP2, and IBA-1 in cortex and striatum brain tissue from WT mice and R6/2 HD mice with different treatments (× 400 magnification). Bar graph shows the optical density (mean) statistical analysis of the changes among various experimental groups. FUS exposure level was set to 14W. ANOVA combined with post-hoc Tukey test was performed for comparisons. Compared with the WT group: single pound, $P < 0.05$; double pounds, $P < 0.01$; compared with the HD sham group: single asterisk, $P < 0.05$; double asterisks, $P < 0.01$. Values are presented as means ± SD. N = 3–6 mice/group.

(2.5 ± 0.7/3.5 ± 0.7) were shown in GDNFp-LPs + FUS treated R6/2 HD mice compared to sham (19.1 ± 1.4/18.0 ± 2.8), reducing approximately 87% and 81% of Htt aggregates in cortex and striatum when compared to the sham group. Cellular apoptosis levels were analyzed by quantifying caspase 3 and TUNEL staining (Fig. 4C 3rd to 6th columns). Positive immunostaining with caspase 3 was observed in the nucleus and cytoplasm and TUNEL-positive apoptotic signals identified in the nucleus. In GDNFp-LPs + FUS group, a slightly increased immunoreactivity for caspase 3 in either the cortex or striatum was found when compared to WT mice, but was significantly lower than the HD sham group. TUNEL immunostaining in striatum was significantly decreased in GDNFp-LPs + FUS group compared to WT and HD sham mice, respectively. These results imply that cellular apoptosis was effectively relieved after GDNFp-LPs + FUS treatment.

In addition, to further investigate whether impairments in motor function correlate with histological changes in the cortex and striatum regions, we next examined the neuronal survival marker P-CREB and oxidative stress marker MDA (Fig. 4C 7th to 10th columns). Administration with GDNFp-LPs following FUS-BBB opening produced a statistically significant increase ($^{**}P < 0.01$) in expression of P-CREB in R6/2 HD mice brains compared to the sham group. To confirm the change in oxidative stress in the brain tissues, MDA was immunoprecipitated. MDA levels in the neural rostral region were significantly higher in the group of GDNFp-LPs + FUS treated R6/2 HD mice than the sham animal group ($^{*}P < 0.05$). Oxidative stress levels contributed to be higher in the sham, GDNFp-LPs, and FUS groups, but the differences were not statistically significant when compared to the WT group. Both markers showed significant improvements with GDNFp-LPs + FUS exposure. This confirmed that GDNFp-LPs + FUS treatment provides the most significant neuronal protection.

Fig. 4D shows fluorescent-tagged immunohistochemistry (IHC) microscopies, to observe cellular changes in neurons and glia in the cortex and striatum regions. Double-labeled IHC staining (green: β-tubulin III and MAP2 to identify neurons; red: GFAP and IBA-1 to respectively identify astroglia and microglia; blue: DAPI to mark all cell nuclei) was performed and merged to demonstrate neuroprotective effects in neuronal cells. β-tubulin exhibited distinct fibrillary cytoskeletal localizations in the cortex and striatum area (1st and 2nd columns). GFAP, an intermediate filament protein, is expressed mainly in astrocytes. β-tubulin staining was associated with neuronal microtubule, whereas GFAP staining was filamentous and distinct from that encountered with β-tubulin. β-tubulin expression was able to induce a preferential growth and branching of neurites in GDNFp-LPs + FUS groups when compared to other groups. GFAP immunoreactivity was elevated in the sham and GDNFp-LPs groups. Of note, GFAP expression was relatively moderate in the GDNFp-LPs + FUS treatment group and close to that of the WT group, implying the neuro-inflammatory response in R6/2 HD mice was lessened. The intensity of microglial marker, IBA-1, in the cortex and striatum area was relatively high in WT and GDNFp-LPs + FUS animals compared to the other groups. This showed that microglia were more activated [38]. Furthermore, MAP2, indicating neurite outgrowth, increased significantly in GDNFp-LPs + FUS animals, and also was very similar to cell types from WT mice. The results confirm that successful GDNF gene delivery and GDNF overexpression provides neuroprotection effects, including neuronal viability and promoting neurite outgrowth.

FUS CNS gene delivery improved motor performance and rescued brain atrophy in HD transgenic mice

Next, we demonstrate the neuroprotective effect via FUS-BBB opening to facilitate CNS GDNF-gene (GDNFp-LPs) delivery into the R6/2 HD mice. Fig. 5A shows R6/2 HD mice developed neuroanatomical changes in various experimental conditions. Significant differences in motor coordination restoration were noted in the GDNFp-LPs + FUS treated group when compared to the sham group. Fig. 5B shows weekly rotarod motor performance among groups. Of note, GDNFp-LPs + FUS provided the most significant improvement of motor ability maintaining through the treatment period from 14- to 18-weeks of age when compared to the other groups. At week 18, a significant difference can be observed when compared GDNFp-LPs + FUS (latency: 201.13 ± 83.56 s) to sham (39.78 ± 28.74 s), GDNFp-LPs only (22.15 ± 0.49 s), and FUS only groups (18.30 ± 20.17 s). The results demonstrated that R6/2 HD mice with GDNFp-LPs and FUS-BBB opening treatment could provide a neuroprotective effect to retard disease progression evidenced by neuroanatomical and motor function observation.

Discussion

Our work demonstrates that FUS exposure-gene therapy enhances neuroprotective effects through successful FUS + MBs-induced GDNF overexpression with the mechanism summarized in Fig. 6. FUS + MBs-enhanced GDNF transduction is shown to be capable of reversing motor deficits, brain rostral atrophy, and neuronal dysfunction and loss. The FUS + MBs-GDNF gene delivery also increases CREB phosphorylation. P-CREB enhances neuronal plasticity and cell survival, which is demonstrated by reduced expression of the antiapoptotic protein caspase 3 and DNA fragmentation (TUNEL). In addition, GDNF overexpression decreases MDA expression, an oxidative stress marker (Fig. 4C and D). We have also shown that the proposed system effectively enhances neurotrophic factor synthesis in the HD brain and provides neuroprotective effects.

Our preclinical evidence supports the hypothesis that FUS + MBs-enhanced GDNF gene delivery can rescue motor impairments and partially retard HD progression, supporting the conclusion that the strategy of FUS + MBs-gene therapy is effective in controlling hereditary disease progression such as HD caused by specific gene mutation might be possible. With its noninvasive feature, FUS-BBB opening system provides opportunity in capable of repetitively and locally delivering therapeutic gene into the brain, for example, HD disease progression control demonstrated in this study.

This study reveals correlations between regional brain atrophy and motor dysfunction via motor performance and MR images from early to late stage of HD (see Supplementary Results S1). Progressive brain atrophy in the cerebral cortex, ventricle, and striatum was compatible with motor deficits, suggesting that changes in brains of MRI may predict neuronal dysfunction. The intracellular aggregates are present in brains of HD mice at 6 weeks of age and increase with over time. These results suggest that the functional change in R6/2 HD mice may have originated from loss of cortex and striatum neurons. Thus, neuroimaging measures might feasibly serve as biomarkers for evaluating the efficacy of neuroprotective treatments in preclinical trials.

GDNF contributes to the growth, development, and plasticity of selective striatal neurons for their survival and/or differentiation [39–41]. GDNF can be delivered in a non-invasive manner to the brain through the BBB using a systemic administration route. Previous work has shown that pDNA encapsulated in neutral stealth liposomes functionalized within a targeting region provides efficient and specific gene delivery *in vivo* [26,30]. The characteristic liposomes (LPs) (Fig. 2) were prepared with three different amounts of pDNA, including GDNF, HttQ25, and HttQ109 as previously described [26,30,31]. The prepared LPs had an average effective diameter of 150 nm, as measured by DLS, with a negative

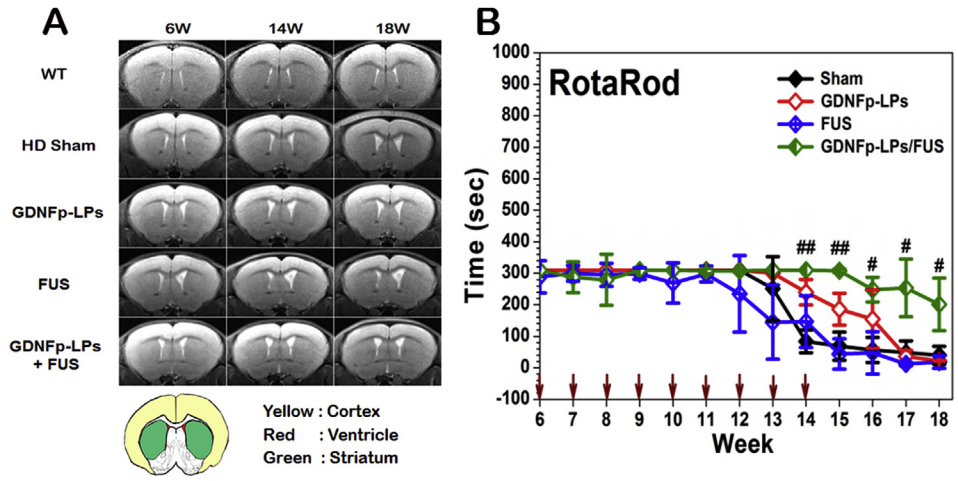

Fig. 5. (A) Representative MR images of a progressive neurological phenotype with or without treatments to show the neuroanatomical changes for the WT, the sham, the GDNFp-LPs only, the FUS only, and the GDNFp-LPs + FUS system groups in R6/2 HD mice. (B) Motor performance via rotarod test under various experimental groups. Measurements of latency time until fall are from the beam walking test. ANOVA combined with post-hoc Tukey test was performed for comparisons. Compared with the HD sham group: single pound, $P < 0.05$; double pounds, $P < 0.01$. Values are presented as means ± SD. $N \geq 6$ mice/group.

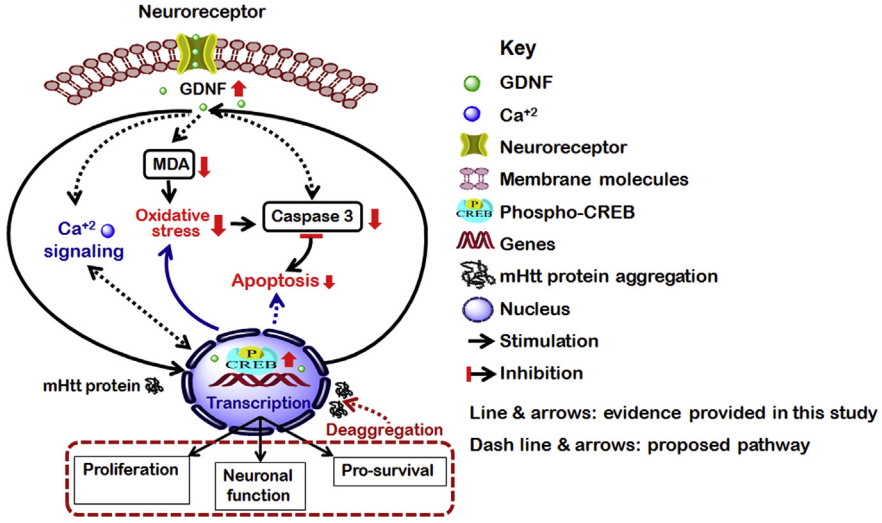

Fig. 6. Schematic representation of the main signaling pathways involved in the neuroprotective action of GDNF on mutant Htt protein aggregation in HD neurons. The FUS-GDNF targets might include ultrasound-induced GDNF overexpression that increase CREB phosphorylation; P-CREB activators that enhance neuronal plasticity and cell survival; CREB transcription factors that alleviate expression of the antiapoptotic protein caspase 3 and DNA fragmentation (TUNEL); FUS modulators that increase GDNF expression; and MDA promotion that decreases cellular oxidative stress.

charge. As shown in Fig. 2B, HttQ25 was homogeneously expressed in nearly all N2A cells transfected with L-HttQ25 using US exposure, whereas nearly all N2A cells transfected with L-HttQ109 using US exposure demonstrated intracellular aggregates. This confirms the possibility in using ultrasound to successfully enhance cell transfection, and using ultrasound as a gene transfection tool for efficient gene delivery *in vivo*.

We also examined how vascular permeability might change due to ultrasound-BBB opening in different disease stages. The assumption is that an intact neurovasculature structure can be altered at different disease stages, potentially affecting the effectiveness of FUS to open the BBB. An excellent correlation can be found between local vascular permeability and enhanced delivery in the early-middle-stages. However, such increase is not found in 18-week-old R6/2 HD mice, which may be due to no significant increase in BBB permeability after FUS exposure with MBs. This is consistent to our observation that MRI kinetic responses reflect a slow perfusion rise effect at the BBB-opened region, particularly in older diseased mice, implying that the FUS may not effectively enhance sufficient diffusivity transition from the vasculature to brain tissues, and this heterogeneous permeability enhancement may hamper therapeutic efficacy in late HD stage. This may suggest that different vascular impairment in different disease stages might be responsible for the heterogeneous effects of FUS exposure with MBs on permeability in HD brain [15]. Therefore, BBB opening through FUS exposure in the presence of MBs can enhance vascular permeability and deposit therapeutics in the targeted tissue to significantly improve treatment efficacy in early HD stage rather than late stage.

This study investigates whether FUS + MBs-gene therapy can facilitate HD therapy through evaluating motor function maintenance. Through 9 weeks of treatment, GDNFp-LPs + FUS treated

mice were indistinguishable with WT mice in motor performance, demonstrating that GDNF-mediated neuroprotective effects can maintain motor function during the entire course of treatment, providing strong evidence of retarding HD progression (see supplementary Results S2) [32,34,42,43]. The synergistically applied FUS + MBs-induced GDNF gene transduction and overexpression retarded HD progression. This result supports that the reversibility of the pathology can be achieved in early stage of disease [14,18,19,32,44].

We have shown the feasibility of combining FUS-BBB opening and non-viral gene vector to serve as a HD gene therapy platform. We have identified an effective FUS + MBs-GDNF treatment protocol that can effectively open the BBB for GDNF gene delivery, and our study results suggest that the procedure may restore neuronal function and retard HD progression. For further extending the potential benefit in using this technique to provide long-term and lasting effect, multiple and repetitive sonication under a well-controlled intact exposure condition [45] should be valuable and can be further investigated.

Conflicts of interest

Hao-Li Liu provides technical consulting service for NaviFUS Inc. Taiwan, and he currently holds patents relates to biomedical ultrasound.

Funding source

This work was supported by the Ministry of Science and Technology, Taiwan, with grant nos. 106-2121-E-182-080, 107-2221-E-182-022, and Chang Gung Memorial Hospital, Taiwan, with grant nos. CORPD3E0071, CMRPD2A0033, CMRPG3D0571, CIRPD2E0051, CMRPD2D0111-3, CMRPD2A0033, and CIRPD3E0131-3.

Acknowledgements

The authors also thank the Microscope Core Laboratory, Chang Gung Memorial Hospital, Linkou for their assistance in the experiment.

Appendix A. Supplementary data

Supplementary data to this article can be found online at https://doi.org/10.1016/j.brs.2019.04.011.

References

[1] Scahill RI, Hobbs NZ, Say MJ, Bechtel N, Henley SM, Hyare H, et al. Clinical impairment in premanifest and early Huntington's disease is associated with regionally specific atrophy. Hum Brain Mapp 2013;34:519–29.
[2] Hobbs NZ, Pedrick AV, Say MJ, Frost C, Dar Santos R, Coleman A, et al. The structural involvement of the cingulate cortex in premanifest and early Huntington's disease. Mov Disord 2011;26:1684–90.
[3] Fusco FR, Chen Q, Lamoreaux WJ, Figueredo-Cardenas G, Jiao Y, Coffman JA, et al. Cellular localization of Huntingtin in striatal and cortical neurons in rats: lack of correlation with neuronal vulnerability in Huntington's disease. J Neurosci 1999;19:1189–202.
[4] Schulte J, Littleton JT. The biological function of the Huntingtin protein and its relevance to Huntington's Disease pathology. Curr Trends Neurol 2011;5:65–78.
[5] Huntington's Disease Finkbeiner S. Cold Spring Harb Perspect Biol 2011;3(6).
[6] Demeestere J, Vandenberghe W. Experimental surgical therapies for Huntington's disease. CNS Neurosci Ther 2010;17:705–13.
[7] Drouin-Ouellet J, Sawiak SJ, Cisbani G, Lagace M, Kuan WL, Saint-Pierre M, et al. Cerebrovascular and blood-brain barrier impairments in Huntington's disease: potential implications for its pathophysiology. Ann Neurol 2015;78:160–77.
[8] Lin CY, Hsu YH, Lin MH, Yang TH, Chen HM, Chen YC, et al. Neurovascular abnormalities in humans and mice with Huntington's disease. Exp Neurol 2013;250:20–30.
[9] Hua J, Unschuld PG, Margolis RL, van Zijl PC, Ross CA. Elevated arteriolar cerebral blood volume in prodromal Huntington's disease. Mov Disord 2014;29:396–401.
[10] Zhao Z, Nelson AR, Betsholtz C, Zlokovic BV. Establishment and dysfunction of the blood-brain barrier. Cell 2015;163:1064–78.
[11] Tietz S, Engelhardt B. Brain barriers: crosstalk between complex tight junctions and adherens junctions. J Cell Biol 2015;209:493–506.
[12] Araujo DM, Hilt DC. Glial cell line-derived neurotrophic factor attenuates the excitotoxin-induced behavioral and neurochemical deficits in a rodent model of Huntington's disease. Neuroscience 1997;81:1099–110.
[13] Sari Y. Huntington's disease: from mutant Huntingtin protein to neurotrophic factor therapy. Int J Biomed Sci 2011;7:89–100.
[14] Alberch J, Perez-Navarro E, Canals JM. Neurotrophic factors in Huntington's disease. Prog Brain Res 2004;146:195–229.
[15] Di Pardo A, Amico E, Scalabri F, Pepe G, Castaldo S, Elifani F, et al. Impairment of blood-brain barrier is an early event in R6/2 mouse model of Huntington Disease. Sci Rep 2017;7:41316.
[16] Weiss N, Miller F, Cazaubon S, Couraud PO. The blood-brain barrier in brain homeostasis and neurological diseases. Biochim Biophys Acta 2009;1788:842–57.
[17] Weis J, Saxena S, Evangelopoulos ME, Kruttgen A. Trophic factors in neurodegenerative disorders. IUBMB Life 2003;55:353–7.
[18] Ramaswamy S, Kordower JH. Gene therapy for Huntington's disease. Neurobiol Dis 2012;48:243–54.
[19] Alberch J, Pérez-Navarro E, Canals JM. Neuroprotection by neurotrophins and GDNF family members in the excitotoxic model of Huntington's disease. Brain Res Bull 2002;57:817–22.
[20] Gratacos E, Perez-Navarro E, Tolosa E, Arenas E, Alberch J. Neuroprotection of striatal neurons against kainate excitotoxicity by neurotrophins and GDNF family members. J Neurochem 2001;78:1287–96.
[21] Pineda JR, Rubio N, Akerud P, Urban N, Badimon L, Arenas E, et al. Neuroprotection by GDNF-secreting stem cells in a Huntington's disease model: optical neuroimage tracking of brain-grafted cells. Gene Ther 2006:1–11.
[22] Rangasamy SB, Soderstrom K, Bakay RA, Kordower JH. Neurotrophic factor therapy for Parkinson's disease. Prog Brain Res 2010;184:237–64.
[23] Lapchak PA, Gash DM, Collins F, Hilt D, Miller PJ, Araujo DM. Pharmacological activities of glial cell line-derived neurotrophic factor (GDNF): preclinical development and application to the treatment of Parkinson's disease. Exp Neurol 1997;145:309–21.
[24] Levine RM, Pearce TR, Adil M, Kokkoli E. Preparation and characterization of liposome- encapsulated plasmid DNA for gene delivery. Langmuir 2013;29:9208–15.
[25] Lin CY, Javadi M, Belnap DM, Barrow JR, Pitt WG. Ultrasound sensitive eLiposomes containing doxorubicin for drug targeting therapy. Nanomedicine : NBM (NMR Biomed) 2014;10:67–76.
[26] Lin CY, Hsieh HY, Pitt WG, Huang CY, Tseng IC, Yeh CK, et al. Focused ultrasound- induced blood-brain barrier opening for non-viral, non-invasive, and targeted gene delivery. J Control Release 2015;212:1–9.
[27] White JK, Auerbach W, Duyao MP, Vonsattel JP, Gusella JF, Joyner AL, et al. Huntingtin is required for neurogenesis and is not impaired by the Huntington's disease CAG expansion. Nat Genet 1997;17:404–10.
[28] Chen PY, Wei KC, Liu HL. Neural immune modulation and immunotherapy assisted by focused ultrasound induced blood-brain barrier opening. Hum Vaccines Immunother 2015;11:2682–7.
[29] Fan CH, Lin WH, Ting CY, Chai WY, Yen TC, Liu HL, et al. Contrast-enhanced ultrasound imaging for the detection of focused ultrasound-induced blood-brain barrier opening. Theranostics 2014;4:1014–25.
[30] Lin CY, Hsieh HY, Chen CM, Wu SR, Tsai CH, Huang CY, et al. Non-invasive, neuron-specific gene therapy by focused ultrasound-induced blood-brain barrier opening in Parkinson's disease mouse model. J Control Release 2016;235:72–81.
[31] Fan CH, Lin CY, Liu HL, Yeh CK. Ultrasound targeted CNS gene delivery for Parkinson's disease treatment. J Control Release 2017;261:246–62.
[32] Burgess A, Huang Y, Querbes W, Sah DW, Hynynen K. Focused ultrasound for targeted delivery of siRNA and efficient knockdown of Htt expression. J Control Release 2012;163:125–9.
[33] Fan CH, Chang EL, Ting CY, Lin YC, Liao EC, Huang CY, et al. Folate-conjugated gene-carrying microbubbles with focused ultrasound for concurrent blood-brain barrier opening and local gene delivery. Biomaterials 2016;106:46–57.
[34] Timbie KF, Mead BP, Price RJ. Drug and gene delivery across the blood-brain barrier with focused ultrasound. J Control Release 2015;219:61–75.
[35] Huang Y, Alkins R, Schwartz ML, Hynynen K. Opening the blood-brain barrier with MR imaging-guided focused ultrasound: preclinical testing on a trans-human skull porcine model. Radiology 2017;282:123–30.
[36] Shen WB, Anastasiadis P, Nguyen B, Yarnell D, Yarowsky PJ, Frenkel V, et al. Magnetic enhancement of stem cell-targeted delivery into the brain following MR-guided focused ultrasound for opening the blood-brain barrier. Cell Transplant 2017;26:1235–46.
[37] Song KH, Harvey BK, Borden MA. State-of-the art of microbubbl-assisted blood-brain barrier disruption. Theranostics 2018;8:4393–408.
[38] Leinenga G, Gotz J. Scanning ultrasound removes amyloid-beta and restores memory in an Alzheimer's disease mouse model. Sci Transl Med 2015;7:278ra33.

[39] Hoffer BJ, Hoffman A, Bowenkamp K, Huettl P, Hudson J, Martin D, et al. Glial cell line-derived neurotrophic factor reverses toxin-induced injury to midbrain dopaminergic neurons in vivo. Neurosci Lett 1994;182:107–11.
[40] Kim BT, Rao VL, Sailor KA, Bowen KK, Dempsey RJ. Protective effects of glial cell line-derived neurotrophic factor on hippocampal neurons after traumatic brain injury in rats. J Neurosurg 2001;95:674–9.
[41] Pérez-Navarro E, Arenas E, Reiriz J, Calvo N, Alberch J. Glial cell line-derived neurotrophic factor protects striatal calbindin-immunoreactive neurons from excitotoxic damage. Neuroscience 1996;75:345–52.
[42] Zeron MM, Hansson O, Chen N, Wellington CL, Leavitt BR, Brundin P, et al. Increased sensitivity to N-Methyl-D-Aspartate receptor-mediated excitotoxicity in a mouse model of Huntington's disease. Neuron 2002;33:849–60.
[43] Stack EC, Del Signore SJ, Luthi-Carter R, Soh BY, Goldstein DR, Matson S, et al. Modulation of nucleosome dynamics in Huntington's disease. Hum Mol Genet 2007;16:1164–75.
[44] Littrell OM, Granholm A-C, Gerhardt GA, Boger HA. Glial cell-line derived neurotrophic factor (GDNF) replacement attenuates motor impairments and nigrostriatal dopamine deficits in 12-month-old mice with a partial deletion of GDNF. Pharmacol Biochem Behav 2013;104:10–9.
[45] Tsai HC, Tsai CH, Chen WS, Inserra C, Wei KC, Liu HL. Safety evaluation of frequent application of microbubble-enhanced focused ultrasound blood-brain-barrier opening. Sci Rep 2018;8:17720.